FEBS Letters 588 (2014) 1154–1160

journal homepage: www.FEBSLetters.org

Crystal structure analysis of EstA from *Arthrobacter* sp. Rue61a – an insight into catalytic promiscuity

Ulrike Gabriella Wagner [a,*], Frank DiMaio [b], Stephan Kolkenbrock [c,1], Susanne Fetzner [c]

[a] Institute of Molecular Biosciences, University of Graz, A-8010 Graz, Austria
[b] Biochemistry Department, University of Washington, Box 357350, Seattle, WA 98195, USA
[c] Institute of Molecular Microbiology und Biotechnology, University of Münster, D-48149, Germany

ARTICLE INFO

Article history:
Received 19 September 2013
Revised 11 February 2014
Accepted 15 February 2014
Available online 5 March 2014

Edited by Stuart Ferguson

Keywords:
Catalytic promiscuity
Crystal structure
Esterase
β-Lactamase
Steric hindrance

ABSTRACT

In this article we analyze the reasons for catalytic promiscuity of a type VIII esterase with β-lactamase fold and the ability to cleave β-lactams. We compared the structure of this enzyme to those of an esterase of the same type without any lactamase ability, an esterase with moderate lactamase ability, and a class C β-lactamase with similar fold. Our results show that for these enzymes, the difference in the substrate specificity is sterically driven.

1. Introduction

Catalytic promiscuity – the ability of enzymes to catalyze distinctly different chemical transformations – is a rather common feature, which is striking as we used to generally associate enzymes with the ability to perfectly stabilize the transition state of one particular chemical reaction. However, the potential for promiscuity may be the key to the evolution of new enzymes, giving nature the starting point to optimize catalysis of a promiscuous reaction. This may also have practical implications on biocatalysis, as studying catalytic promiscuity is likely to expand our knowledge on enzymes used for organic synthesis.

Catalytic promiscuity might be due to the enzyme's capability to mediate different catalytic mechanisms, or to accept different functional groups of substrates, or both. The largest group of proteins showing catalytic promiscuity involves enzymes active towards analogous functional groups, like esters and β-lactams/amides where the bonds broken (C–O versus C–N) differ but the molecular reaction mechanisms are similar. Differences are found in the direction of the nucleophile attack in relation to the leaving group: *syn* in esters/amides, but *anti* in lactams/lactones. This has an impact for the placement of the general acid donating a proton to the departing group [1]. Another striking difference is the pK_a value of the leaving group: with a pK_a of ~15 the leaving alcohol may be displaced either as an anion or as alcohol while a pK_a of ~25 for amines requires protonation [2]. Therefore esters may be cleaved even in the absence of a properly oriented general acid.

Both enzyme classes – esterases as well as β-lactamases – exhibit a high degree of molecular and functional diversity. Based on conserved sequence motifs and properties, esterases are classified into eight families [3], with family VIII showing significant similarity to β-lactamases on the sequence level as well as concerning structure. According to the most accepted classification scheme defined by Ambler [4] and later extended by Jaurin and Grundstrom [5] and Ouellette et al. [6], β-lactamases are divided into four classes – A, B, C and D. Assignment depends on the presence of specific signatures or motifs. In the above mentioned scheme, sequences of class C β-lactamases contain three conserved elements S-X-S-K, Y-S-N and K-T-G at position 64, 150 and 314 (numbering refers to AmpC), respectively [7–9]. According to this

Abbreviations: $EstA_A$, carboxylesterase from *Arthrobacter* sp. Rue61a; $EstB_{Bg}$, carboxylesterase from *Burkholderia gladioli*; $P99_{Ec}$, class C β-lactamase from *Enterobacter cloacae*; EstU1, metagenome derived carboxylesterase; 2NB, 2-naphthylbutyrate; PenG, penicillin G

* Corresponding author. Address: University of Graz, Institute of Molecular Biosciences/Structural Biology, Humboldtstrasse 50/III, A-8010 Graz, Austria. Fax: +43 316 3809897.
E-mail address: ulrike.wagner@uni-graz.at (U.G. Wagner).
[1] Present address: evocatal GmbH, Alfred-Nobel-Str. 10, 40789 Monheim, Germany.

http://dx.doi.org/10.1016/j.febslet.2014.02.045
0014-5793/

classification, the esterases of family VIII employed in this study are most closely related to class C β-lactamases.

Carboxylesterase from *Arthrobacter* sp. Rue61a ($EstA_A$) was previously described as a family VIII esterase active towards short-chain phenylacyl esters [10]. However, it is also able to moderately catalyze the hydrolysis of β-lactams. A microiodometric assay that depends on the reduction of iodine by penicilloic acid [11] suggested specific activities of His_6-$EstA_A$ of about 0.1 U mg^{-1} towards penicillin G, and 0.2 U mg^{-1} towards 6-aminopenicillanic acid. Even if such activities are by factors of several thousand lower than the activity of $EstA_A$ observed for hydrolysis of phenylacetyl ester (about 700 U mg^{-1}), this is about the same order of magnitude as described for the recently published promiscuous metagenome derived carboxylesterase (EstU1) [12]. Penicillin G and 6-aminopenicillanic acid (K_i = ~800 μM) moreover act as weak competitive inhibitors of $EstA_A$ against phenylacetic acid, indicating that these β-lactams bind to the active site. Table S1 gives an overview of kinetic parameters of the four enzymes used in this study.

In this work, we describe the crystal structure of $EstA_A$ and compare it with the structures of the already published esterase carboxylesterase from *Burkholderia gladioli* ($EstB_{Bg}$) [13] which shows no activity against β-lactams, the class C β-lactamase from *Enterobacter cloacae* ($P99_{Ec}$) – a "true" lactamase [14], and EstU1 [12]. The aim of this study was to broaden our knowledge of catalytic promiscuity.

2. Materials and methods

2.1. Production of recombinant $EstA_A$ protein

$EstA_A$, encoded by the ARUE_c39440 locus of *Arthrobacter* sp. Rue61a [15], was produced as His_6-tagged protein in *Escherichia coli* BL21 [pLysS, pET23aKm-*estA*]. In this expression plasmid, the ampicillin resistance gene of the pET23a(+) backbone was replaced by the *aphIII* gene conferring kanamycin resistance. The EstA-His_6 protein was purified as reported previously [10].

2.2. Crystallization, data collection, structure determination and refinement

Crystals of $EstA_A$ were obtained through mixing 1 μl of protein (10 mg/ml) with 1 μl of precipitant solution containing 0.1 M Tris buffer (pH 5.5), 0.2 M sodium chloride and 25% PEG 3350 at 20 °C. Drops were covered with a 2:1 mixture of Dow corning oil: paraffin oil. Crystals appeared after 1 day and reached their final size after 2–3 days. Diffraction data were collected at the EMBL outstation at DESY (Deutsches Elektronen Synchrotron) in Hamburg, Germany, beamline X12 on a Mar Mosaic 225 detector. Data were processed using XDS [16] and Scala [17].

Structure solution of $EstA_A$ was performed employing molecular replacement with phenix.mr_rosetta [18]. The missing parts were built in Coot [19] and structure refinement was carried out with Refmac [20] and Buster [21], alternately manual model building and minimization to produce the final model (R_f = 0.181, R_{free} = 0.216) (Table 1).

2.3. Docking experiments

We tried soaking experiments utilizing various possible ligands but did not succeed in getting interpretable electron density. To study the differences between our three model enzymes with regard to ligand binding we therefore docked 2-naphthylbutyrate (2NB) as well as penicillin G (PenG) into our model structures using the Schrödinger program package [22]. The first substrate was chosen because it is known that $EstB_{Bg}$ hydrolyzes this ester. On the other hand, $EstA_A$ reacts slowly with penicillin G. The structures of the two ligands were built and refined in Maestro [22]. Covalent docking experiments were performed with Glide [22] using a box-size slightly larger than the model ligand and extra precision option for docking. The obtained solutions were refined with Prime [22]. Ranking of solutions was done with conformation search in MacroModel [22] using only the ligand substructure. Interaction fingerprint [23] was used to score the poses corresponding to the number of interactions between the enzyme and the substrate.

Table 1
Data collection and refinement statistics of $EstA_A$.

Wavelength (Å)	0.88557
Resolution range (Å)	135–2.45 (2.51–2.45)
Space group	$I4_132$
Molecules/asymmetric unit	1
Unit cell dimensions	
a, *b*, *c* (Å)	191.25
α, β, γ (°)	90
Total reflections	455184
Unique reflections	25288
Reflections used in refinement (>2σ)	20988
Multiplicity	17.2 (18.2)
Completeness (%)	99.62 (99.88)
Mean I/σ (I)	8.30 (1.80)
Wilson B-factor (Å^2)	46.8
R_{sym}	0.08 (0.44)
R-factor	0.181
R_{free}	0.216
Number of atoms	3011
Macromolecules	2855
Ligands	9
Water	147
Protein residues	372
RMS bonds (Å)	0.023
RMS angles (°)	2.05
Ramachandran favored (%)	96.22
Ramachandran outliers (%)	6.01
Clashscore	12.67
Average B-factor (Å^2)	32.98
Macromolecules	32.56
Solvent	39.38
Ligand	63.81

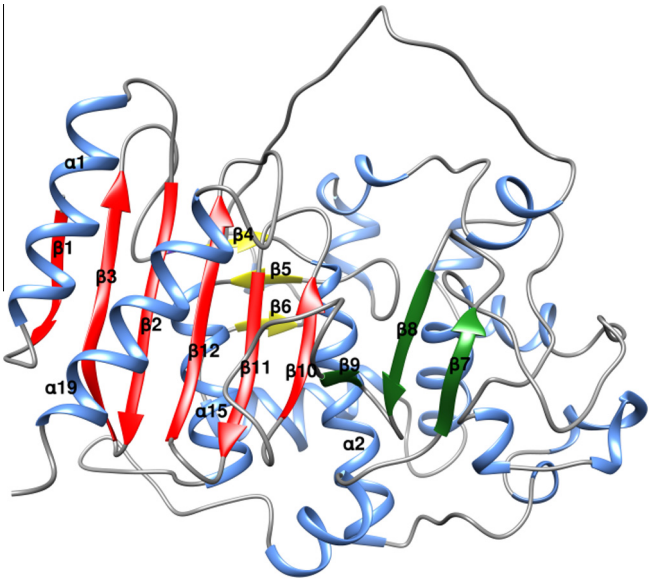

Fig. 1. Ribbon representation of $EstA_A$. Coloring according to secondary structure: red (sheet A), green (sheet B), yellow (sheet C); helices are in blue. Only the β-strands and the helices flanking sheet B are labeled.

The highest scored poses were applied to compare the ligand bindings between the model enzymes. 2NB produced reasonable results with all our model proteins, whereas PenG gave positive results only with $P99_{Ec}$ and $EstA_A$.

3. Results and discussion

3.1. Crystal structure of $EstA_A$

The structure of $EstA_A$ was determined at 2.45 Å. All residues are reflected in the electron density (Fig. S1) although some loop regions are poorly defined (Fig. S2). Like the other two known type VIII esterase structures, the structure of $EstA_A$ is composed of two domains: the central α/β domain (from residue 1–77 and 169–372) and a structurally more flexible domain, consisting of mainly helices and loops (residues 78–168). The α/β domain is composed of three antiparallel β-sheets (A–C). Sheet A consists of seven β-strands (β1–β3 and β9–β12), B of three β-strands (β4–β6) and C of two β-strands (β7 and β8). Sheet A and C form the central β-sheet while B roughly extends this sheet in the length but is approximately vertical to it. Two α-helices (α1 and α19) cover the large β-sheet from one side, five helices (α2, α9, α10, α11 and the 3_{10} helix α15) form the other. In addition the central domain is built up by three α-helices (α12, α14 and α17) and three 3_{10} helices (α14, α16 and α18). The helical domain is comprised of four α-helices (α5, α6, α7, α8) and two 3_{10} helices (α3 and α4). Fig. 1 shows a ribbon model of $EstA_A$ colored by secondary structure elements.

```
EstA_A      1 ---MHS-QVIAPG---F-EPVAELFGVFLEQDPD---Y-SAQVAAYHRGVKVLDLSGGPH
EstB_Bg     3 ---------AASL---A-ARLDAVFDQALRERRL---V-GAVAIVARHGEILYRRAQGLA
P99_Ec      2 -PV-----SEKQL---A-EVVANTITPLMKAQSV---P-GMAVAVIYQGKPHYYTFGKAD
EstU1      25 --AEGPVTATKPKEAGFTSEGLARIDAYLKNEIQAKTMPGAVMMIKRNGETAYFSSFGLR

EstA_A     49 -------IRP-DSVTGVFSCSKGMAGLVMALLVQDGELDLEAEVVKYWPEFGVE------
EstB_Bg    58 DREAGRPMRE-DTLFRLASVTKPIVALAVLRLVARGELALDAPVTRWLPEFRPRLA--DG
P99_Ec     47 --IAANKPVTPQTLFELGSISKTFTGVLGGDAIARGEISLDDPVTRYWPQLTGK------
EstU1      83 DPDTKEPMTA-ETIFRIYSMSKPITTVAAMMLVEEGKLQLDEPVSKYIPSFANVKVGVET

EstA_A     95 -----------GK-SSITVAQLLSHRA-GLL-G----------V-EGGLT---LHEVNNS
EstB_Bg   115 -----------SE-PLVTIHHLLTHTS-GLG-YWLLEGAGSV-YDRLGISDGIDLRDFDL
P99_Ec    120 -----------QW-QGIRMLDLATYTAGGLP-L----------Q-VPDEV----TD---N
EstU1     142 KGENGMALETGPVKRAITIQDLMRHTS-GITYGFVGDGLVKKAY-IASNLF---DGDFDN

EstA_A    127 ELAAAKLAELPPLWKPGTAFGYHALTIGIFMEELCRRITGSTLQEVFEQRIRAVTGA-NF
EstB_Bg   160 DENLRRLASAPLSFAPGSGWQYSL--ALDVLGAVVERATGQPLAAAVDALVAQPLGM-RD
P99_Ec    128 ASLLRFYQNWQPQWKPGTTRLYANASIGLFGALAVKPSGMPYEQAMTTRVLKPLKLD-HT
EstU1     197 AEFAERIAKLPLVYQPGTTWDYGHSTDILGRVVEVVSGKSLYQFEKERLLDPLGM---KD

EstA_A    187 YLGLPES-EESRFAQFRWAAD---P------SWPWV-DPASHFGLAANAAVGDILDLPNIR
EstB_Bg   218 CGFVSA--EPERFAVPYHDGQPEPVRMRDGIEVPLPE----GHG--A-A---V-FAPSRVF
P99_Ec    190 WINVPKA-EEAHYAWGYRDGK----------------------------------AV-
EstU1     256 TGFYVTDPAKKSLVAEAMPND---R-------K-------------I-G--GS--EMFDPR

EstA_A    238 EVRAAGLSSAAGVASAEGMARIYAAALTGLEGKSAMPPLLTEETIRTVSAEQV----FGID
EstB_Bg   268 EPGAYPSGGAGMYGSADDVLRALEAIRAN-------PGFLPETLADAARRDQA----GVGA
P99_Ec    217 PGM-LDAQAYGVKTNVQDMANWVMANMAPE----NVADASLKQGIALAQSRYW----RIG-
EstU1     289 VQKKWEPGGQGMVSTIGDYARFTQMVLNGGTL-DGKRYLSPKTIAYMGSNHIPQASGIVPG

EstA_A    289 RVFG-ET-GCFGTVFMKS-------H----T-RM-PF--------------------GSYR
EstB_Bg   318 ETRG-PG-WGFGYLSAVL-------D---DPAAAGTP--------------------QHAG
P99_Ec    267 ------S-MYQGLGWEMLNWPVEANT----V-VE-GSDSKVALAPLPVAEVNPPAPPVKAS
EstU1     349 AYYLPGPGVGFGLGFAVR-------TEAG-V-TP-VE--------------------GSVG

EstA_A    321 AFGHDGA--SASLGFADPVYELGFGYVPQTAEPGGVGCRNFQLSSAVRE      364
EstB_Bg   346 TLQWGGV--YGHSWFVDRALGLSVLLLTNTAYEGMSGPLTIALRDAVYA      391
P99_Ec    316 WVHKTGSTGGFGSYVAFIPEKQIGIVMLANTSYPN-P-A-RVEAAYHIL      366
EstU1     380 DLSWGGA--GGTVFWIDPKENLTVVFMAPMVSPRA--RVWRTLRNIVYG      422
```

Fig. 2. Sequence alignment based on the structure of the four enzymes of our model system. Structural alignments were done with LSQMAN [38]. The three conserved motifs are marked with a box.

Table 2
Pairwise sequence comparison of esterases and β-lactamase $P99_{Ec}$. Identities and similarities for structurally aligned proteins were calculated using the server http://www.bioinformatics.org/sms/multi_align.html, and using the BLAST algorithm. The score of pairwise comparisons between the four aligned structures was calculated with SSM [37].

Alignment based on structure				BLAST sequence alignment			SSM	
		Identity (%)	Positive (%)	Identity (%)	Positive (%)	Coverage[a] (%)	rmds	N_{align}
$EstA_A$	$EstB_{Bg}$	20	31	28	45	30	2.71	284
$EstA_A$	$P99_{Ec}$	12	23	23	47	43	2.77	277
$EstA_A$	EstU1	16	30	24	48	46	2.72	312
$EstB_{Bg}$	$P99_{Ec}$	15	26	24	39	79	2.29	292
$EstB_{Bg}$	EstU1	25	36	30	46	89	1.86	333
$P99_{Ec}$	EstU1	15	25	25	42	47	2.39	304

[a] Coverage lower than 50% comprises only to the N-terminal part.

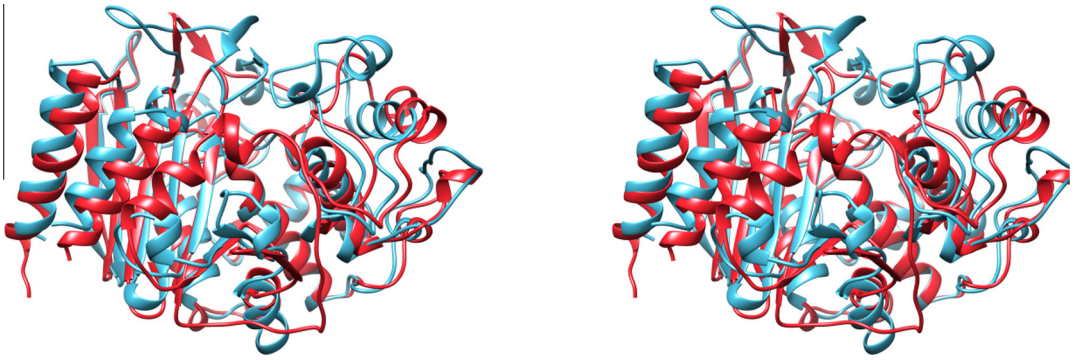

Fig. 3. Stereo view of a structural alignment made with matchmaker (program package Chimera) for $EstB_{Bg}$ (blue) and $P99_{Ec}$ (red).

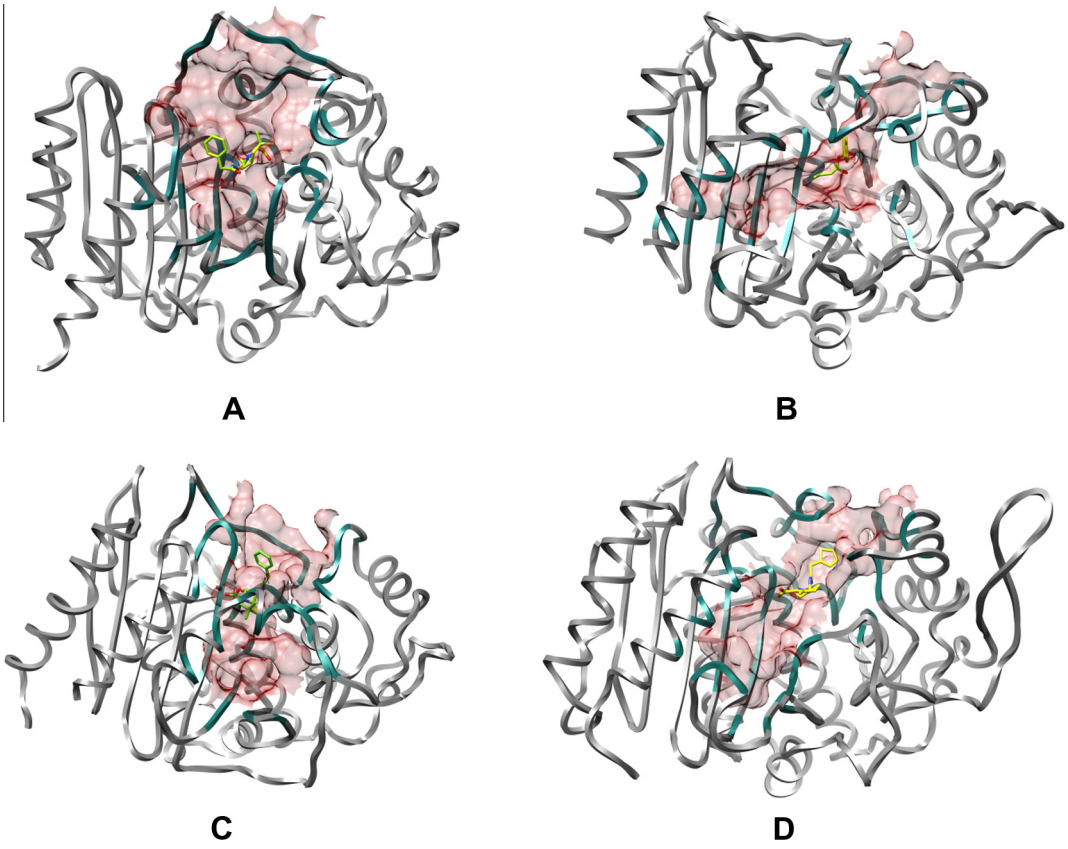

Fig. 4. Ribbon representation with surface of binding pockets calculated with CASTp for $EstA_A$ (A), $EstB_{Bg}$ (B), $P99_{Ec}$ (C) and EstU1 (D). Ligands are shown in yellow (2NB in $EstB_{Bg}$, PenG in $EstA_A$ and $P99_{Ec}$ and cephalothin in EstU1). The R1 site refers to the upper part of the binding pocket, the R2 site to the lower one.

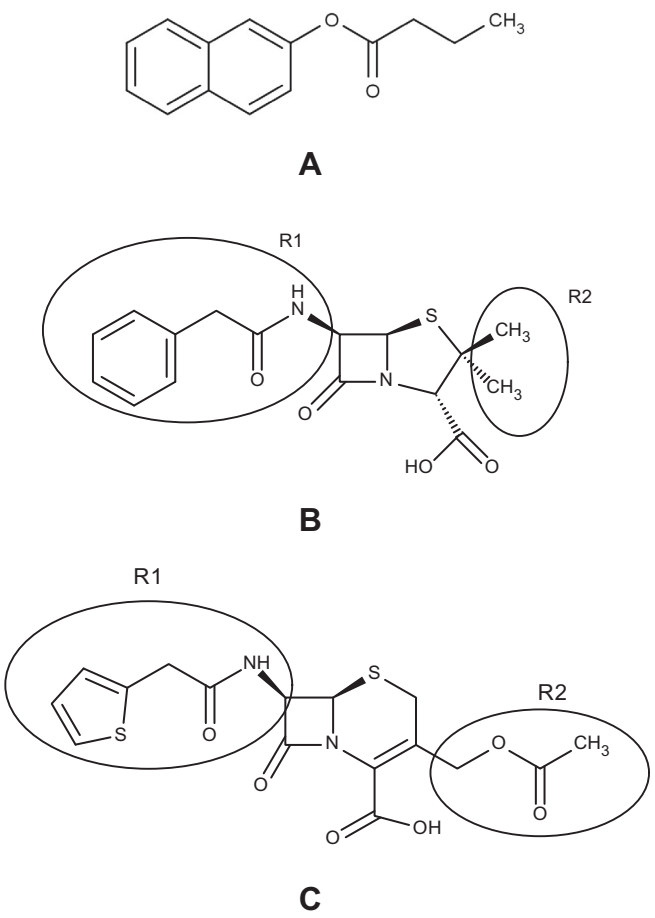

Fig. 5. Chemical structures of 2-naphthyl butyrate (A), penicillin G (B) and cephalothin (C). The moieties of penicillin and cephalothin that are recognized by the R1 and R2 subsites of the enzymes (cf. Fig. 4) are marked.

Table 3
Quantification of pockets and mouths calculated with CASTp.

Enzyme	P-area[a]	P-vol[b]	M-area[c]	M-circ[d]
$EstB_{Bg}$	1088	1302	177	119
$EstA_A$	1198	2512	351	121
$P99_{Ec}$	1072	1546	279	118
EstU1	1574	2385	280	151

[a] Pocket area based on solvent-accessible surface in Å^2.
[b] Pocket volume based on solvent-accessible surface in Å^3.
[c] Total area of mouth opening based on solvent-accessible surface Å^2.
[d] Total circumference of mouth opening based on molecular surface Å.

3.2. Sequence alignment of $EstA_A$, $EstB_{Bg}$, EstU1, and β-lactamase $P99_{Ec}$

The carboxylesterases EstU1, $EstB_{Bg}$ and the N-terminal part of $EstA_A$ (to about residue 190) exhibit low but significant sequence similarities to each other as well as to class C β-lactamases. Contrarily, no protein structure resembles the C-terminal part of $EstA_A$ on the sequence level. Fig. 2 shows a multiple alignment of the amino acid sequences of our model enzymes based on structural alignment and Table 2 lists the percentage of identical and similar residues. The three characteristic motifs of class C β-lactamases are not completely conserved: in the first motif (S-X-S-K), which comprises the active-site serine and a lysine also involved in the enzymatic mechanism, $EstB_{Bg}$ has the serine adjacent to the lysine replaced by a threonine. For the second and third motif (Y-S-N and K-T-G), only the tyrosine of motif 2 and the glycine at the last position of motif 3 are conserved. But it could be shown that only the serine in the first and the tyrosine in the second motif are essential for enzymatic activity: the hydroxyl of serine acts as the catalytic nucleophile and tyrosine is supposed to act as a general base [24–26]. Both lysines, in motif one as well as in motif three, enhance the enzymatic reaction [27,28]. However, it was also proven that the same applies for other basic amino acids in the first position of the third motif [27].

3.3. Overall comparison of the structures of $EstA_A$, $EstB_{Bg}$, EstU1, and β-lactamase $P99_{Ec}$

In contrast to the low overall sequence identity between $EstA_A$ and other esterases or β-lactamases (Table 2), the three dimensional structures show a high degree of conservation. A search for proteins structurally similar to $EstA_A$ using Matras [29] revealed structurally highly related proteins with approximately the same score: EstU1 as most closely related, followed by $EstB_{Bg}$ and several β-lactamases, D-amino acid amidases, trans-esterases and DD-carboxypeptidases, supporting the assumption that $EstA_A$ and EstU1 represent structural links between esterases of type VIII and β-lactamases. Fig. 3 illustrates the similarity between our model structures.

To find out which regions of the protein are evolutionarily most conserved, the structure of $EstA_A$ was sent to the ConSurf server [30,31]. The graphical representation of the result is shown in Fig. S3b. Apparently the core exhibits a high degree of conservation while the periphery of the active site appears to be highly flexible. A similar finding emerges from the patch point distance calculation between $EstA_A$-$P99_{Ec}$, $EstA_A$-$EstB_{Bg}$ and $EstA_A$-EstU1 using Vasco [32]. The results are shown in Fig. S3c–e. Striking structural differences are predominantly found in regions forming the active site and the entrance to it.

As already pointed out for EstU1 [33], the main reason for substrate discrimination between our model proteins is the difference concerning the active site conformation(s). Fig. 4 shows a ribbon representation of all structures with binding pockets calculated by CASTp [34]. The active site can be divided into two subsites: the R1 site hosts the side chain bound to the lactam ring, and the R2 site binds the substituents or side chain bound to the 5 or 6 membered ring fused to the lactam ring (Fig. 5) [35]. The shape of the binding pocket differs significantly between the proteins. In $P99_{Ec}$ the access to the R1 site is only restricted by the Ω-loop (residues 199–218) thus leaving enough space for bulkier substrates to enter. Contrarily, a β-sheet (residues 245–259) completely covers the R1 site of $EstB_{Bg}$. In $EstA_A$ a loop (residues 199–214) limits the size of accepted substrates, and three loops (residues 171–179, 188–195 and 274–286) impede the access to the R1 site in EstU1. The accessibility to the R2 site also shows significant differences: easiest accessibility is found in EstU1 where only a loop formed by residues 345–354 covers part of the pocket. $EstB_{Bg}$ shows a shorter loop (residues 310–321) in the same place resulting in less entrance coverage. The shapes of the entrances to the active site of $EstB_{Bg}$ and EstU1 are similar-nearly rectangular-making it difficult for bulky substrates to enter. The binding pocket of $EstA_A$ is widely open to the front, reflected by the larger mouth volume compared to that of EstU1, with both showing approximately the same pocket volume (Table 3). The active site of $P99_{Ec}$ is unique, formed as a large tunnel closed to the front by a helix-loop-helix motif (residues 283–296). Sheet C, also present in all structures, is tilted out of the plane of the central β-sheet to open the access to the R1 site. But in $EstA_A$ this sheet is longer and has a much smaller tilt, thus covering the R1 site. As a conclusion, in our model structures not only the size of R1 and R2 sites differs, but also the location and size of the entrances to the active site (Fig. S4).

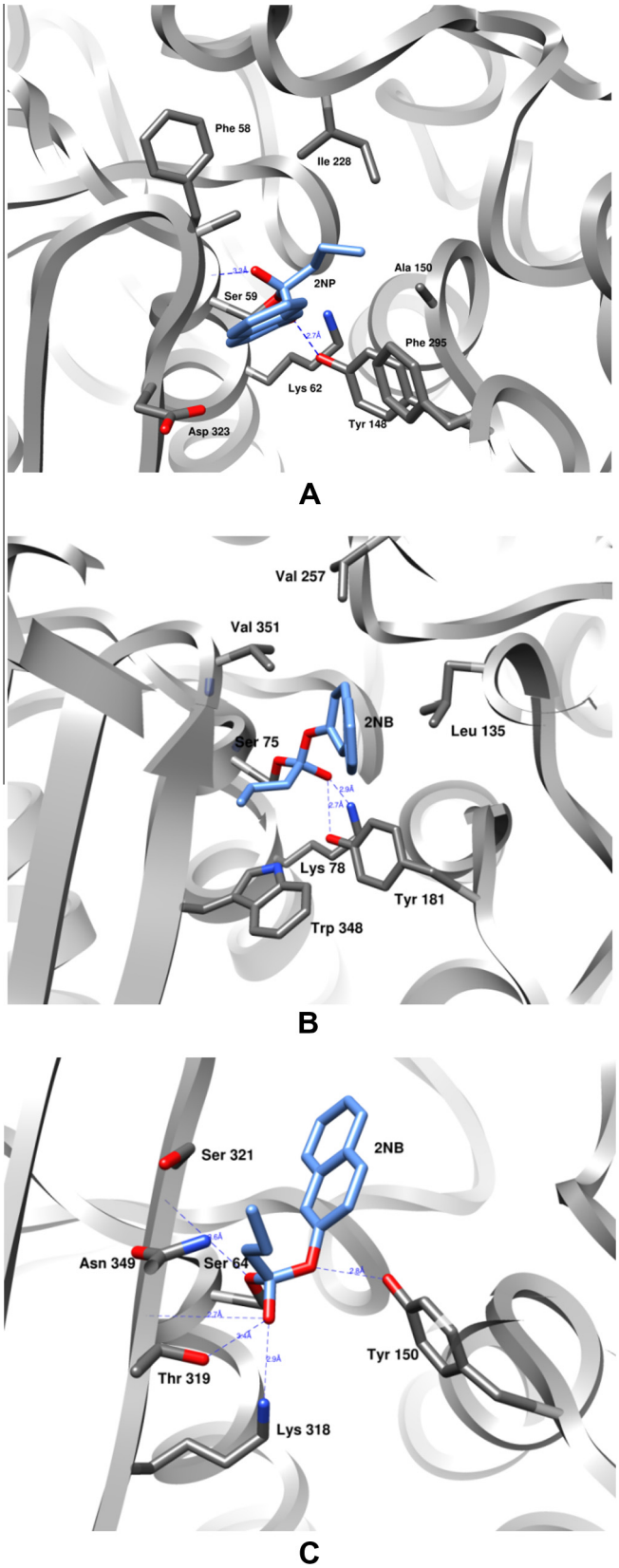

Fig. 6. Active site of $EstA_A$ (A), $EstB_{Bg}$ (B) and $P99_{Ec}$ (C) with docked substrate (2NB).

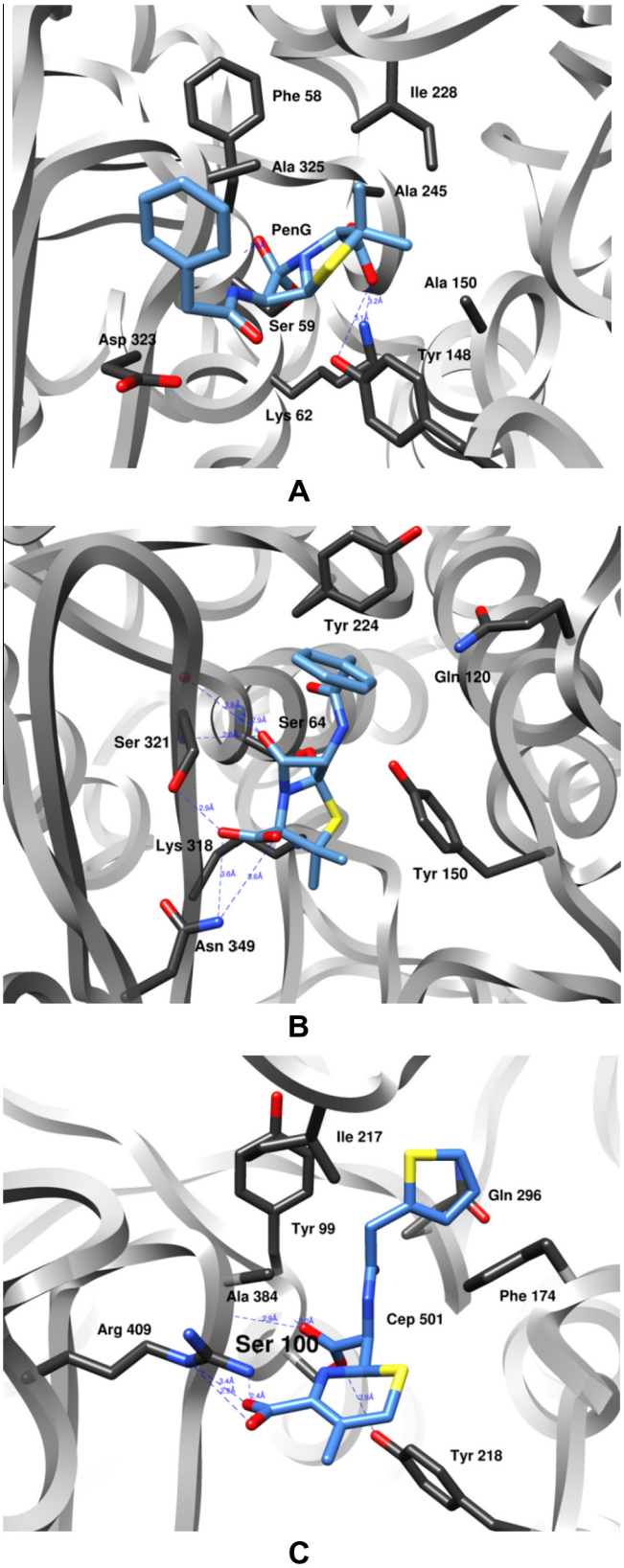

Fig. 7. Active site of $EstA_A$ (A) and $P99_{Ec}$ (B) with docked penicillin G as substrate. For comparison EstU1 (**C**) with bound cephalothin is also shown.

3.4. Comparison of bound substrates in the active sites

A close-up look at the active sites of $EstA_A$, $EstB_{Bg}$, and $P99_{Ec}$ with 2NB as docked substrate (Fig. 6) clearly reveals the differences in binding: while the substrate is stabilized by hydrogen bonds as well as hydrophobic interactions in the two esterases, the large binding pocket of $P99_{Ec}$ makes it impossible to utilize hydrophobic interactions for substrate stabilization.

For $EstA_A$ and $P99_{Ec}$ we also performed docking experiments with penicillin G (Fig. 7). While the substrate in $P99_{Ec}$ as expected binds according to the R1–R2 rule [36], a loop (res 221–229) makes such an arrangement impossible in $EstA_A$. This could be one of the reasons for the weak β-lactamase activity of $EstA_A$.

Following the observations described above we can conclude that for our model enzymes the major discriminating factors for substrate acceptance are the size of the active site pocket and the entrance to it.

Accession number

The coordinates and structure factors for $EstA_A$ have been deposited in the Protein Data Bank (PDB: 3ZYT).

Acknowledgements

We thank Prof. Jean-Marie Frère and Prof. M. Nukaga for providing us with $P99_{Ec}$. UGW thanks Silvia Wallner and Judith Kerstner for useful discussions.

Appendix A. Supplementary data

Supplementary data associated with this article can be found, in the online version, at http://dx.doi.org/10.1016/j.febslet.2014.02.045.

References

[1] Page, M.I. (1991) The energetics of intramolecular reactions and enzyme catalysis. Philos. Trans. R. Soc. Lond. B Biol. Sci. 332, 149–156.
[2] Rhazi, N., Galleni, M., Page, M.I. and Frère, J.-M. (1999) Peptidase activity of β-lactamases. Biochem. J. 341, 409–413.
[3] Arpigny, J.L. and Jaeger, K.-E. (1999) Bacterial lipolytic enzymes: classification and properties. Biochem. J. 343, 177–183.
[4] Ambler, R.P. (1980) The structure of β-lactamases. Philos. Trans. R. Soc. Lond. B Biol. Sci. 289, 321–331.
[5] Jaurin, B. and Grundstrom, T. (1981) AmpC cephalosporinase of *Escherichia coli* K-12 has a different evolutionary origin from that of β-lactamases of the penicillinase type. Proc. Natl. Acad. Sci. USA 78, 4897–4901.
[6] Ouellette, M., Bissonnette, L. and Roy, P.H. (1987) Precise insertion of antibiotic resistance determinants into Tn21-like transposons: nucleotide sequence of the OXA-1 β-lactamase gene. Proc. Natl. Acad. Sci. USA 84, 7378–7382.
[7] Matagne, A., Lamotte-Brasseur, J. and Frère, J.M. (1998) Catalytic properties of class A β-lactamases: efficiency and diversity. Biochem. J. 330 (Pt 2), 581–598.
[8] Singh, R., Saxena, A. and Singh, H. (2009) Identification of group specific motifs in β-lactamase family of proteins. J. Biomed. Sci. 16, 109–115.
[9] Goldberg, S.D., Iannuccilli, W., Nguyen, T., Ju, J. and Cornish, V.W. (2003) Identification of residues critical for catalysis in a class C β-lactamase by combinatorial scanning mutagenesis. Protein Sci. 12, 1633–1645.
[10] Schütte, M. and Fetzner, S. (2007) EstA from *Arthrobacter nitroguajacolicus* Rü61a, a thermo- and solvent-tolerant carboxylesterase related to class C β-lactamases. Curr. Microbiol. 54, 230–236.
[11] Novick, R.P. (1962) Microiodometric assay for penicillinase. Biochem. J. 83, 236–240.
[12] Cha, S.S., An, Y.J., Jeong, C.S., Kim, M.K., Jeon, J.H., Lee, C.M., Lee, H.S., Kang, S.G. and Lee, J.H. (2013) Structural basis for the β-lactamase activity of EstU1, a family VIII carboxylesterase. Proteins 81, 2045–2051.
[13] Petersen, E.I., Valinger, G., Sölkner, B., Stubenrauch, G. and Schwab, H. (2001) A novel esterase from *Burkholderia gladioli* which shows high deacetylation activity on cephalosporins is related to β-lactamases and dd-peptidases. J. Biotechnol. 89, 11–25.
[14] Lobkovsky, E., Moews, P.C., Liu, H., Zhao, H., Frère, J.M. and Knox, J.R. (1993) Evolution of an enzyme activity: crystallographic structure at 2-Å resolution of cephalosporinase from the *ampC* gene of *Enterobacter cloacae* P99 and comparison with a class A penicillinase. Proc. Natl. Acad. Sci. USA 90, 11257–11261.
[15] Niewerth, H., Schuldes, J., Parschat, K., Kiefer, P., Vorholt, J.A., Daniel, R. and Fetzner, S. (2012) Complete genome sequence and metabolic potential of the quinaldine-degrading bacterium *Arthrobacter sp.* Rue61a. BMC Genomics 13, 534.
[16] Kabsch, W. (2010) XDS. Acta Crystallogr. D Biol. Crystallogr. 66, 125–132.
[17] Evans, P.R. (2011) An introduction to data reduction: space-group determination, scaling and intensity statistics. Acta Crystallogr. D Biol. Crystallogr. 67, 282–292.
[18] DiMaio, F., Terwilliger, T.C., Read, R.J., Wlodawer, A., Oberdorfer, G., Wagner, U., Valkov, E., Alon, A., Fass, D., Axelrod, H.L., Das, D., Vorobiev, S.M., Iwai, H., Pokkuluri, P.R. and Baker, D. (2011) Improved molecular replacement by density- and energy-guided protein structure optimization. Nature 473, 540–543.
[19] Emsley, P., Lohkamp, B., Scott, W.G. and Cowtan, K. (2010) Features and development of Coot. Acta Crystallogr. D Biol. Crystallogr. 66, 486–501.
[20] Murshudov, G.N., Vagin, A.A. and Dodson, E.J. (1997) Refinement of macromolecular structures by the maximum-likelihood method. Acta Crystallogr. D Biol. Crystallogr. 53, 240–255.
[21] Blanc, E., Roversi, P., Vonrhein, C., Flensburg, C., Lea, S.M. and Bricogne, G. (2004) Refinement of severely incomplete structures with maximum likelihood in BUSTER-TNT. Acta Crystallogr. D Biol. Crystallogr. 60, 2210–2221.
[22] L. Schrödinger, Schrödinger Package, New York, 2009.
[23] Deng, Z., Chuaqui, C. and Singh, J. (2004) Structural interaction fingerprint (SIFt): a novel method for analyzing three-dimensional protein–ligand binding interactions. J. Med. Chem. 47, 337–344.
[24] Oefner, C., D'Arcy, A., Daly, J.J., Gubernator, K., Charnas, R.L., Heinze, I., Hubschwerlen, C. and Winkler, F.K. (1990) Refined crystal structure of β-lactamase from *Citrobacter freundii* indicates a mechanism for β-lactam hydrolysis. Nature (London, UK) 343, 284–288.
[25] Lobkovsky, E., Billings, E.M., Moews, P.C., Rahil, J., Pratt, R.F. and Knox, J.R. (1994) Crystallographic structure of a phosphonate derivative of the *Enterobacter cloacae* P99 cephalosporinase: mechanistic interpretation of a β-lactamase transition-state analog. Biochemistry 33, 6762–6772.
[26] Dubus, A., Ledent, P., Lamotte-Brasseur, J. and Frère, J.-M. (1996) The roles of residues Tyr150, Glu272, and His314 in class C β-lactamases. Proteins Struct. Funct. Genet. 25, 473–485.
[27] Tsukamoto, K., Nishida, N., Tsuruoka, M. and Sawai, T. (1990) Function of the conserved triad residues in the class C β-lactamase from *Citrobacter freundii* GN346. FEBS Lett. 271, 243–246.
[28] Tsukamoto, K., Tachibana, K., Yamazaki, N., Ishii, Y., Ujiie, K., Nishida, N. and Sawai, T. (1990) Role of lysine-67 in the active site of class C β-lactamase from *Citrobacter freundii* GN346. Eur. J. Biochem. 188, 15–22.
[29] Kawabata, T. (2003) MATRAS: a program for protein 3D structure comparison. Nucleic Acids Res. 31, 3367–3369.
[30] Ashkenazy, H., Erez, E., Martz, E., Pupko, T. and Ben-Tal, N. (2010) ConSurf 2010: calculating evolutionary conservation in sequence and structure of proteins and nucleic acids. Nucleic Acids Res. 38, W529–533.
[31] Goldenberg, O., Erez, E., Nimrod, G. and Ben-Tal, N. (2009) The ConSurf-DB: pre-calculated evolutionary conservation profiles of protein structures. Nucleic Acids Res. 37, D323–327.
[32] Steinkellner, G., Rader, R., Thallinger, G.G., Kratky, C. and Gruber, K. (2009) VASCo: computation and visualization of annotated protein surface contacts. BMC Bioinformatics 10, 32.
[33] Sun-Shin, C., Young Jun, A., Chang-Sook, J., Min-Kyu, K., Jeong Ho, J., Chang-Muk, L., Hyun, S.L., Sung, G.K. and Lee, J.-H. (2013) Structural basis for the β-lactamase activity of EstU1, a family VIII carboxylesterase. Proteins, http://dx.doi.org/10.1002/prot24334.
[34] Dundas, J., Ouyang, Z., Tseng, J., Binkowski, A., Turpaz, Y. and Liang, J. (2006) CASTp: computed atlas of surface topography of proteins with structural and topographical mapping of functionally annotated residues. Nucleic Acids Res. 34, W116–118.
[35] Kim, J.Y., Ha Il, J., Young, J.A., Jung, H.L., So, J.K., Seok, H.J., Kye, J.L., Pann-Ghill, S., Heung-Soo, L., Sang, H.L. and Sun-Shin, C. (2006) Structural basis for the extended substrate spectrum of CMY, a plasmid-encoded class C β-lactamase. Mol. Microbiol. 60, 907–916.
[36] Jeon, J.H., Kim, S.J., Lee, H.S., Cha, S.S., Lee, J.H., Yoon, S.H., Koo, B.S., Lee, C.M., Choi, S.H., Lee, S.H., Kang, S.G. and Lee, J.H. (2011) Novel metagenome-derived carboxylesterase that hydrolyzes β-lactam antibiotics. Appl. Environ. Microbiol. 77, 7830–7836.
[37] Krissinel, E. and Henrick, K. (2004) Secondary-structure matching (SSM), a new tool for fast protein structure alignment in three dimensions. Acta Crystallogr. D Biol. Crystallogr. 60, 2256–2268.
[38] Kleywegt, G.J. and Jones, T.A. (1995) Where freedom is given, liberties are taken. Structure 3, 535–540.